

Front-end Replication Dynamic Window (FRDW) for Online Motor Imagery Classification

Xinru Chen, Jiayu An, Huanyu Wu, Siyang Li, Bin Liu, and Dongrui Wu

Abstract—Motor imagery (MI) is a classical paradigm in electroencephalogram (EEG) based brain-computer interfaces (BCIs). Online accurate and fast decoding is very important to its successful applications. This paper proposes a simple yet effective front-end replication dynamic window (FRDW) algorithm for this purpose. Dynamic windows enable the classification based on a test EEG trial shorter than those used in training, improving the decision speed; front-end replication fills a short test EEG trial to the length used in training, improving the classification accuracy. Within-subject and cross-subject online MI classification experiments on three public datasets, with three different classifiers and three different data augmentation approaches, demonstrated that FRDW can significantly increase the information transfer rate in MI decoding. Additionally, FR can also be used in training data augmentation. FRDW helped win national champion of the China BCI Competition in 2022.

Index Terms—Brain-computer interface, dynamic window, electroencephalogram, motor imagery, online classification

I. INTRODUCTION

A brain-computer interface (BCI) can measure and process the subject's brain activities and translate them into interactive information or commands for external device control [1]. Sensorimotor rhythm (SMR) based BCIs [2]–[4] are based on the principle that the execution or imagination of limb movements, the latter also known as motor imagery (MI), changes the cortical rhythmic activity [5]. The increase and decrease of the SMR are called event-related synchronization (ERS) and event-related desynchronization (ERD), respectively.

Electroencephalogram (EEG) can record SMR changes during MI, which can be used for BCI control [6]–[8]. MI-based BCIs are achieved by imagining the movement of a specific body part, e.g., left hand, right hand, feet, or tongue, without actually performing it [9]. They have been used in wheelchair/robot control, stroke rehabilitation, gaming, etc [10]–[14].

MI classification could be performed offline or online. Offline classification means the entire test EEG data are available offline for analysis. Online classification collects the subject's EEG signals and makes inferences in real-time, aiming at both high classification accuracy and fast response. The information transfer rate (ITR) is an important metric for online BCIs.

X. Chen, J. An, H. Wu, S. Li and D. Wu are with the Ministry of Education Key Laboratory of Image Processing and Intelligent Control, School of Artificial Intelligence and Automation, Huazhong University of Science and Technology, Wuhan 430074, China. They are also with the Shenzhen Huazhong University of Science and Technology Research Institute, Shenzhen, China.

B. Liu is with Beijing Fenghuo Wanjia Technology Co. Ltd., Beijing, 100026, China.

X. Chen and J. An contributed equally to this work.

D. Wu is the corresponding author (e-mail: drwu09@gmail.com).

There are several challenges for online MI classification:

- 1) *Varying EEG trial length.* Most EEG classification algorithms assume the input trial has a fixed length, whereas for fast response, EEG trials in online classification usually have varying lengths.
- 2) *Trade-off between speed and accuracy.* For fast response, classifications should be made for short EEG trials, which usually reduces the accuracy.
- 3) *Large individual differences.* In cross-subject MI classification, to alleviate individual differences, some EEG data from the test subject are usually needed for model calibration. Online classification usually has less calibration data than offline classification.

To cope with these challenges, we propose a front-end replication dynamic window (FRDW) approach for online MI classification. Our main contributions are:

- 1) We propose a front-end replication (FR) approach to fill each test EEG trial to a fixed length required by the online classifier, improving the classification accuracy. Additionally, FR can also be used in training data augmentation.
- 2) We use a dynamic window (DW) approach to adaptively adjust the length of each test EEG trial to improve the decoding speed.
- 3) We integrate Euclidean alignment (EA) [15] with FRDW to accommodate individual differences in online cross-subject MI classification.

Extensive within- and cross-subject experiments on three public MI datasets with three classifiers and three data augmentation approaches demonstrated the effectiveness of our proposed FRDW approach. FRDW helped win national champion of the China BCI Competition in 2022¹.

The remainder of this paper is organized as follows: Section II introduces related works. Section III describes the FRDW approach. Section IV introduces the experimental settings. Section V presents the experimental results. Finally, Section VI draws conclusions.

II. RELATED WORKS

This section introduces related works on offline MI classification, online MI classification, and DW approaches for EEG classification.

¹<http://www.worldrobotconference.com/cn/view/1938.html>

A. Offline MI Classification

Both conventional machine learning and deep learning (DL) have been used in offline EEG-based MI classification.

Conventional machine learning typically uses expert knowledge to extract EEG features and then feeds them into a traditional classifier, e.g., support vector machine (SVM). Common spatial pattern (CSP) [16] and its variants, e.g., sparse CSP [17], L1-norm-based CSP [18], divergence CSP [19], and probabilistic CSP [20], have been widely used in MI signal processing and feature extraction. Filter bank CSP [21] first partitions the EEG signal into different frequency bands, and then applies CSP to each of them. Some studies also used power spectral density [22], [23] or wavelet transform [24] features.

Most DL approaches take raw EEG signals as the input. Popular convolutional neural network (CNN) based DL approaches include EEGNet [25], Deep ConvNet [26] and Shallow ConvNet [26]. EEG-TCNet [27], TCNet-Fusion [28], and ATCNet [29] are their enhancements by temporal convolution, fusion layer, and attention. Filter bank multi-scale CNN (FBMSNet) [30] extends filter bank from traditional learning to DL.

B. Online MI Classification

Online MI classification has been attracting much attention, due to the requirement of real-time BCIs.

Yang *et al.* [31] applied data augmentation to the first three-second of a test trial to get five samples, and then voted the five real-time predictions for the final result. The average binary classification accuracy on 80 test trials from two subjects was 71.3%. Tayeb *et al.* [32] controlled the movement of a robotic arm in real-time, which only responded to high-confidence predictions. Parashiva *et al.* [33] trained an Error-Related Potential detection model to learn the brain response to feedback and make automatic corrections, achieving 64.88% online classification accuracy. Furthermore, asynchronous MI [34], [35] first recognizes whether the subject is performing MI, and then makes classification. Its typical performance measure includes both classification accuracy and ITR.

C. Dynamic Window for EEG Classification

DWs were introduced to alleviate the limitations of fixed windows (FWs). They have found applications in online Steady-State Visual Evoked Potential (SSVEP) based BCIs.

Spatiotemporal equalization DW recognition [36] allows the adaptive control of the stimulus timing while maintaining high recognition accuracy, significantly improving the ITR and the system's adaptability to different subjects. Chen *et al.* [37] proposed a filter bank canonical correlation analysis based training-free DW recognition approach for SSVEP. Hadi *et al.* [38] proposed a novel DW classifier, using ensembling learning for SSVEP recognition. [39], [40] enhanced DW threshold selection to further improve the ITR for SSVEP classification. DL-based DW has also been used in SSVEP recognition, e.g., Zhou *et al.* [41] proposed an EEGNet-DW approach, which uses a different EEGNet model and threshold for each DW length.

To our knowledge, there has not been DW approaches for MI-based BCIs.

III. METHODOLOGY

This section introduces our proposed FRDW algorithm. The Python code is available at <https://github.com/XinRu2001/FRDW>.

A. Problem Setting

Assume we have trained an MI classifier $f(X)$, where $X \in \mathbb{R}^{C \times N}$, in which C is the number of EEG channels, and N the fixed trial length. During the test stage, n test trials $\{X'_i\}_{i=1}^n$ arrive one by one. For each test trial, each sampling update brings in L' points, i.e., each test trial arrives in the sequence of dimensionality $\mathbb{R}^{C \times L'}$, $\mathbb{R}^{C \times 2L'}$, \dots , $\mathbb{R}^{C \times N}$. For maximum ITR, we should make an accurate classification as early as possible, not necessarily waiting for the full $X'_i \in \mathbb{R}^{C \times N}$.

B. FRDW for Online Within-Subject MI Classification

We propose FRDW to improve the ITR of MI-based BCIs.

A DW on the test dataflow acts on the currently available test trial data $X' \in \mathbb{R}^{C \times L}$, where $\underline{L} \leq L \leq N$ and \underline{L} is the minimum length. When $L < N$, FR is used to fill X' to length N to match the trial length used in training. Specifically, X' is repeatedly concatenated:

$$\overline{X} = [X', X', \dots, X']. \quad (1)$$

\overline{X} is then trimmed to have N columns and used as the input to the classifier. This approach is called FR because trimming keeps the front-end of X' .

When the maximum classification probability on the current \overline{X} is lower than a confidence threshold τ , the current window may be too short for reliable classification. In such case, we wait for another L' samples, and apply FR to the test input of length $L + L'$. The process is repeated until the maximum classification probability exceeds or equals τ . In the worst-case scenario, the entire test trial of length N is used for classification.

Algorithm 1 gives the pseudo-code of FRDW for online within-subject MI classification.

C. FRDW with EA for Online Cross-Subject MI Classification

In cross-subject MI classification, FRDW can be combined with EA [15] for better performance. EA aligns EEG trials from different subjects in the Euclidean space to reduce individual differences, improving the transfer learning performance on a new subject [42].

Assume there are n trials $\{X_i\}_{i=1}^n$ from a subject. EA first computes the reference matrix \overline{R} as the arithmetic mean of all n covariance matrices:

$$\overline{R} = \frac{1}{n} \sum_{i=1}^n X_i X_i^\top. \quad (2)$$

Each trial X_i is then aligned by

$$\tilde{X}_i = \overline{R}^{-1/2} X_i, \quad i = 1, \dots, n \quad (3)$$

Algorithm 1: FRDW for online within-subject MI classification.

Input: $X' \in \mathbb{R}^{C \times L}$, the current test trial;
 \underline{L} , the minimum trial length;
 $(p, m) = f(X)$, the classifier, where
 $X \in \mathbb{R}^{C \times N}$, p is the maximum prediction probability,
and m is the predicted class;
 τ , the confidence threshold.

Output: m , the predicted class.

while $L < N + L'$ **do**
 if $L < \underline{L}$ **then**
 $L \leftarrow L + L'$;
 Get $X' \in \mathbb{R}^{C \times L}$ from the dataflow;
 else if $\underline{L} \leq L < N$ **then**
 Construct \bar{X} using (1);
 $(p, m) \leftarrow f(\bar{X})$;
 if $p \geq \tau$ **then**
 return m .
 else
 $L \leftarrow L + L'$;
 Get $X' \in \mathbb{R}^{C \times L}$ from the dataflow;
 end
 else
 $(p, m) \leftarrow f(X_N)$, where X_N contains the first
 N points of X' ;
 return m .
 end
end

where \tilde{X}_i is the aligned sample for X_i .

After EA, the mean covariance matrix of each subject equals the identity matrix I :

$$\begin{aligned} \frac{1}{n} \sum_{i=1}^n \tilde{X}_i \tilde{X}_i^T &= \bar{R}^{-1/2} \left(\frac{1}{n} \sum_{i=1}^n X_i X_i^T \right) \bar{R}^{-1/2} \\ &= \bar{R}^{-1/2} \bar{R} \bar{R}^{-1/2} = I. \end{aligned} \quad (4)$$

i.e., EEG trials from different subjects become more consistent.

Since EA requires a few EEG trials for calculating the reference matrix \bar{R} , it raises problems at the beginning of the test phase when there are too few test trials. When the number of test trials is smaller than a threshold n_{EA} ($n_{EA} = 10$ in this paper), no EA is performed on the test trials, and a classifier without EA is applied to them. When n_{EA} test trials are accumulated, we compute and save the reference matrix \bar{R} , perform EA on each test trial thereafter, and apply a classifier with EA to it.

Algorithm 2 shows the pseudo-code of FRDW with EA for online cross-subject MI classification.

IV. EXPERIMENTS

Extensive experiments were performed to validate the superior performance of FRDW.

A. Dataset and Preprocessing

Three public MI datasets were used in our experiments, whose statistics are summarized in Table I.

Algorithm 2: FRDW with EA for online cross-subject MI classification.

Input: $X'_n \in \mathbb{R}^{C \times L}$, the current test trial;
 \underline{L} , the minimum trial length;
 $(p, m) = f(X)$, the classifier without EA,
where $X \in \mathbb{R}^{C \times N}$, p is the maximum prediction probability, and m is the predicted class;
 $(p, m) = f_{EA}(X)$, the classifier with EA;
 τ , the confidence threshold;
 n_{EA} , the minimum number of test trials for applying EA;
 $\{X'_i\}_{i=1}^{n-1}$, all test trials before the current trial;
 \bar{R} , the reference matrix of EA; needed only when $n > n_{EA}$.

Output: m , the predicted class.

if $n \leq n_{EA}$ **then**
 $(p, m) \leftarrow f(X'_n)$, where $X'_n \in \mathbb{R}^{C \times N}$;
end

if $n = n_{EA}$ **then**
 Compute \bar{R} on $\{X'_i\}_{i=1}^n$ using (2);
end

if $n \geq n_{EA}$ **then**
 $\tilde{X}'_n \leftarrow \bar{R}^{-1/2} X'_n$;
 while $L < N + L'$ **do**
 if $L < \underline{L}$ **then**
 $L \leftarrow L + L'$;
 Get $X'_n \in \mathbb{R}^{C \times L}$ from the dataflow;
 else if $\underline{L} \leq L < N$ **then**
 Construct \bar{X}_n from \tilde{X}'_n using (1);
 $(p, m) \leftarrow f_{EA}(\bar{X}_n)$;
 if $p \geq \tau$ **then**
 return m .
 else
 $L \leftarrow L + L'$;
 Get $X'_n \in \mathbb{R}^{C \times L}$ from the dataflow;
 end
 else
 $(p, m) \leftarrow f_{EA}(\tilde{X}'_N)$, where \tilde{X}'_N contains
 the first N points of \tilde{X}'_n ;
 return m .
 end
 end
end

All three datasets were from BCI Competition IV [43] and had the same collection protocol. Each subject sat in front of a computer screen. At the beginning of each trial, a fixation cross appeared on the screen, accompanied by a warning tone. Shortly after, an arrow pointing to a particular direction appeared as a cue (e.g., left arrow for left hand, down arrow for feet), prompting the subject to perform the instructed MI task until the fixation cross disappeared from the screen. The next trial started after a short break. EEG signals were recorded during the experiment.

EEG signals in all three datasets were imported from an

TABLE I
STATISTICS OF THE THREE MI DATASETS.

Dataset	# Subjects	# Channels	# Training Trials	# Test Trials	# Classes
MI1	9	22	288	288	4
MI2	9	22	144	144	2
MI3	9	3	400	320	2

open-source repository². Their specific properties are:

- 1) *MI1*. The 22-channel (Fz, FC3, FC1, FCz, FC2, FC4, C5, C3, C1, Cz, C2, C4, C6, CP3, CP1, CPz, CP2, CP4, P1, Pz, P2, POz) EEG signals were sampled at 250 Hz from 9 subjects. Two sessions on different days were recorded for each subject, one for training and the other for test. Each training or test session contained 72 trials per class, and there were four classes (left hand, right hand, feet, and tongue).
- 2) *MI2*. MI2 is identical to MI1, except that it only considered binary classification (left hand and right hand).
- 3) *MI3*. The 3-channel (C3, Cz, C4) EEG signals were sampled at 250 Hz from 9 subjects for binary classification (left hand and right hand). There were three training sessions and two test sessions. The first two training sessions had 60 trials per class without feedback, and the last three sessions had 80 trials per class with smiley feedback.

We detrended the raw full-channel EEG data and used a 5th-order 8-26Hz Butterworth bandpass filter to remove muscle artifacts and direct current drift.

B. Data Augmentation

We used two EEG data augmentation approaches to reduce model overfitting:

- 1) *overlap*. The trials are augmented using sliding windows, i.e., each sliding window contains 25 sampling points of the original data, and there is a 75-point overlap between two successive windows. Note that ‘none’ in our comparison means no overlap between any successive windows was used.
- 2) *FR*. FR introduced in Section III can also be employed for data augmentation in training. It uses sliding windows of length $0.7 * N$ and 25-point overlap to segment each training trial. Then, for each sliding window, FR is used to complement the front-end data to the back, making the total length N .

C. Classifiers

Three classifiers were considered:

- 1) *EEGNet*. EEGNet [25] is a popular CNN for EEG classification. It starts with a temporal convolution followed by a depthwise convolution and a separable convolution, and finally a fully connected layer for classification. We used eight temporal filters and two spatial filters, and dropout rate 0.25.

- 2) *CSP+Transformer*. CSP [16]+Transformer [44] was inspired by Conformer [45], which used a convolutional transformer. However, the data length used by Conformer was about eight times longer than ours, and it is difficult for us to extract features with only two one-dimensional convolutions. Therefore, we utilized CSP to extract log-variance features and performed a temporal convolution and a depthwise convolution on the features as patch embeddings. The transformer encoder block was repeated three times, and a fully connected layer was used for classification. For 4-class MI classification, we used a one-versus-rest strategy for CSP [46], which divided the 4-class classification task into four binary-classification tasks. We concatenated the first four rows of each filter as the final filter.
- 3) *CSP+SVM*. Feature extraction using CSP and then classification using SVM [47] is a classical MI classification approach. We employed radial basis function kernel with regularization parameter $C = 0.1$ for within-subject SVM training, and linear kernel with $C = 1$ for cross-subject SVM training (default values were used for all other parameters).

D. Performance Metric

The ITR, which considers both the classification speed and accuracy, was used as the primary performance metric:

$$\text{ITR} = \frac{60}{T} (\log_2 M + P \log_2 P + (1 - P) \log_2 \frac{1 - P}{M - 1}), \quad (5)$$

where T is the average trial length (s), M the number of classes, and P the classification accuracy. The unit of ITR is bits/min. When $P < \frac{1}{M}$, i.e., the classification accuracy is lower than random, the ITR is set to 0.

Taking four-class classification as an example, the relationship between the ITR and the classification accuracy for different T is shown in Fig. 1. For a fixed T , the ITR grows exponentially as the accuracy increases. For a fixed accuracy, the ITR is an inverse function of the trial length. So, to improve the ITR, we should increase the classification accuracy while reducing the trial length.

E. Experimental Settings

All datasets were partitioned into two parts, training and test. We reserved part of the training data as the validation set, i.e., each class’s last 12 trials (the last block) on MI1 and MI2, and the last 44 trials (20%) on MI3.

For within-subject MI classification, we first recorded the hyper-parameters (e.g., trial length, number of epochs) corresponding to the best ITR on the validation set, and then combined the training and validation sets to train the final model using them. For cross-subject MI classification, we used leave-one-subject-out cross-validation, i.e., the test set of one subject was used for testing and the training sets of all other subjects were combined for training. The model with the best validation ITR was used (no re-training as in the within-subject case).

During offline training, the same data preprocessing and augmentation procedures were applied to the training and

²<http://www.bnci-horizon-2020.eu/database/data-sets>

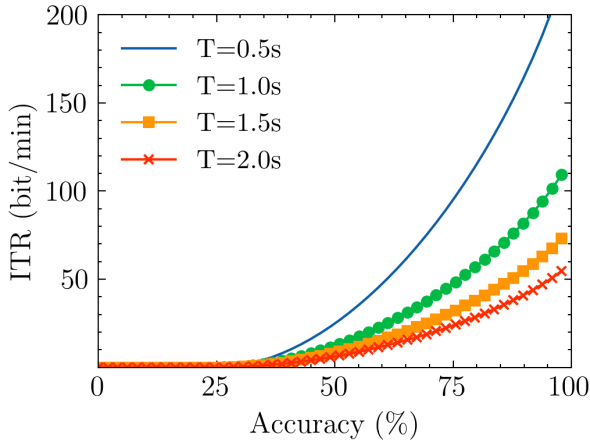


Fig. 1. Relationship between the ITR and classification accuracy for different trial length T .

validation sets. We used the training set to calculate the CSPs, which were then used for validation set feature extraction.

We also used offline data to simulate the online data acquisition process: the EEG data were down-sampled to 250Hz and sent out every 40 ms, i.e., each DW update contained 10 samples ($L' = 10$).

F. Hyper-parameters

There were two types of hyper-parameters: model training related, and FRDW related.

Model training related hyper-parameters included the trial length, FR ratio, maximum number of epochs, learning rate, and batch size. The data length was selected from $\{100, 125, 150, 200, 250, 500, 750\}$ according to the ITR on the validation set. The maximum number of training epochs 100, learning rate 0.001, and batch size 64 were used. To cope with randomness, in each experiment, EEGNet and CSP+Transformer were repeated 11 times, and the average performance was reported. CSP+SVM was run only once, as it was much more stable.

The values of the FRDW related hyper-parameters are shown in Table II.

TABLE II
FRDW RELATED HYPER-PARAMETERS.

Setting	Binary classification		4-class classification	
	\underline{L}	τ	\underline{L}	τ
Within-subject	60	0.7	60	0.6
Cross-subject	60	0.6	50	0.4

V. RESULTS

This section presents the experimental results to demonstrate the effectiveness of FRDW.

A. Online MI Classification

Tables III-V show the ITRs and accuracies (ACCs) in within-subject classification on the three datasets, respectively.

Table III also includes the detailed results on each individual subject. Tables VI-VIII show the ITRs and ACCs in cross-subject classification on three datasets, respectively. The best ITRs for each training data augmentation approach are marked in bold. The values in parentheses are the improvements of FRDW over FW.

Tables III-VIII show that:

- 1) Compared with FW, FRDW improved ITR with little or no loss of accuracy, regardless of the dataset, classifier, and data augmentation approach.
- 2) FR can also be used for data augmentation in training, achieving comparable or better results than others.
- 3) In cross-subject classification (Tables VI-VIII), combining EA with FRDW can further improve the ITR in most cases.

To examine if the differences between FW and our proposed FRDW, and between FRDW without and with EA, were statistically significant, we performed paired-sample t -tests on the ITRs in Tables III-VIII. The null hypothesis was that the difference between the paired samples has zero mean, and it was rejected if $p \leq 0.05$.

The within- and cross-subject paired-sample t -test results between FW and FRDW are shown in Tables IX and X, respectively. The results for FRDW without and with EA are shown in Table XI. The statistically significant ones are marked in bold.

Table IX shows that most p -values were smaller than or close to 0.05 when FR was used for train data augmentation, indicating statistically significant ITR improvement of FRDW over FW in within-subject MI classification. Table X shows that most p -values were smaller than or close to 0.05 when FR and EA were used together, indicating statistically significant ITR improvement of FRDW over FW in cross-subject MI classification.

B. Sensitivity Analysis

Fig. 2 shows the sensitivity analysis results of the two hyper-parameters in FRDW, \underline{L} and τ , on MI1 for within-subject classification.

For a fixed confidence threshold τ , when the minimum trial length \underline{L} increased, generally the ITR first increased and then decreased. For a fixed minimum trial length \underline{L} , when the confidence threshold τ increased, the ITR also first increased and then decreased. Both results are intuitive.

Fig. 2 also shows that FR data augmentation almost always outperformed ‘none’ and ‘overlap’, except when CSP+SVM was used. However, since CSP+SVM generally performed worse than EEGNet and CSP+Transformer, EEGNet with FR or CSP+Transformer with FR is recommended.

C. Ablation Study

Transformer and SVM classifiers do not require the input EEG trial to have a fixed length, so they can also be used without data replication. However, this subsection shows that using FR in testing still improved their ITRs.

Tables XII-XIII show the test results without and with FR when Transformer and SVM were used as the classifier,

TABLE III
ITRS AND ACCURACIES IN WITHIN-SUBJECT CLASSIFICATION ON MI1.

Model	Training Data Augmentation	Test Strategy	Subject									Avg.	
			1	2	3	4	5	6	7	8	9	ITR	ACC
EEGNet	none	FW	76.42	5.43	92.72	36.27	6.57	12.67	67.68	77.72	62.93	48.71	0.54
		FRDW	83.95	5.4	107.46	37.01	6.63	12.79	66.44	90.37	68.19	53.14 ($\uparrow 9.1\%$)	0.53 ($\downarrow 0.01$)
	overlap	FW	95.61	9.62	92.72	39.91	0.01	13.21	83.01	89.89	66.48	54.49	0.55
		FRDW	114.3	8.3	107.64	41.38	0.03	13.48	86.21	89.9	72.78	59.33 ($\uparrow 8.9\%$)	0.53 ($\downarrow 0.02$)
	FR	FW	101.53	8.24	95.61	38.98	0.25	14.34	85.72	94.16	67.68	56.28	0.56
		FRDW	133.37	7.34	119.85	40.07	0.25	14.63	97.19	115.37	70.5	66.51 ($\uparrow 18.2\%$)	0.55 ($\downarrow 0.01$)
CSP+Transformer	none	FW	74.18	14.88	77.66	23.6	1.91	12.4	59.09	73.04	63.22	44.44	0.56
		FRDW	101.19	6.64	99.46	31.09	1.07	13.93	106.79	77.22	77.19	57.18 ($\uparrow 28.7\%$)	0.53 ($\downarrow 0.03$)
	overlap	FW	73.04	12.4	65.33	24.9	0.09	13.37	64.27	78.83	64.27	44.06	0.55
		FRDW	108.9	7.34	90.84	33.13	0.05	13.6	107.64	76.32	73.04	56.76 ($\uparrow 28.8\%$)	0.52 ($\downarrow 0.03$)
	FR	FW	73.04	6.6	78.83	25.57	0.35	18.14	73.04	76.49	64.27	46.26	0.56
		FRDW	123.13	7.63	110.68	34.19	0.79	16.04	111.67	80.6	72.08	61.87 ($\uparrow 33.7\%$)	0.55 ($\downarrow 0.01$)
CSP+SVM	none	FW	56.14	1.71	52.90	37.16	0.06	4.39	32.79	35.40	52.90	30.38	0.47
		FRDW	74.38	1.42	65.44	37.54	0.06	4.39	44.79	34.3	55.09	35.27 ($\uparrow 16.1\%$)	0.46 ($\downarrow 0.01$)
	overlap	FW	64.11	0.97	52.90	34.52	1.31	4.07	33.65	33.65	50.77	30.66	0.47
		FRDW	76.45	0.74	66.31	34.86	1.31	4.11	48.9	34.7	52.34	35.53 ($\uparrow 15.9\%$)	0.46 ($\downarrow 0.01$)
	FR	FW	61.76	0.97	52.90	31.97	0.97	4.73	29.51	33.65	53.95	30.04	0.47
		FRDW	67.8	1.22	67.8	37.16	0.03	3.76	39.46	34.98	55.63	34.20 ($\uparrow 13.8\%$)	0.46 ($\downarrow 0.01$)

TABLE IV
AVERAGE ITRS AND ACCURACIES IN WITHIN-SUBJECT CLASSIFICATION ON MI2.

Model	Training Data Augmentation						
	none		overlap		FR		
	FW	FRDW	FW	FRDW	FW	FRDW	
EEGNet	ITR	21.26	25.91 ($\uparrow 21.9\%$)	25.09	30.11 ($\uparrow 20.0\%$)	24.70	29.76 ($\uparrow 20.5\%$)
	ACC	0.66	0.66 (-)	0.70	0.68 ($\downarrow 0.02$)	0.69	0.68 ($\downarrow 0.01$)
CSP+Transformer	ITR	24.00	34.04 ($\uparrow 41.8\%$)	19.32	32.49 ($\uparrow 68.2\%$)	24.64	33.73 ($\uparrow 36.9\%$)
	ACC	0.70	0.69 ($\downarrow 0.01$)	0.69	0.69 (-)	0.71	0.69 ($\downarrow 0.02$)
CSP+SVM	ITR	25.36	34.97 ($\uparrow 37.9\%$)	25.09	32.45 ($\uparrow 29.3\%$)	24.32	33.92 ($\uparrow 39.5\%$)
	ACC	0.70	0.69 ($\downarrow 0.01$)	0.69	0.68 ($\downarrow 0.01$)	0.69	0.69 (-)

TABLE V
AVERAGE ITRS AND ACCURACIES IN WITHIN-SUBJECT CLASSIFICATION ON MI3.

Model	Training Data Augmentation						
	none		overlap		FR		
	FW	FRDW	FW	FRDW	FW	FRDW	
EEGNet	ITR	21.19	34.10 ($\uparrow 60.9\%$)	23.20	34.05 ($\uparrow 46.8\%$)	22.82	33.81 ($\uparrow 48.2\%$)
	ACC	0.72	0.70 ($\downarrow 0.02$)	0.73	0.70 ($\downarrow 0.03$)	0.73	0.70 ($\downarrow 0.03$)
CSP+Transformer	ITR	26.10	32.11 ($\uparrow 23.0\%$)	27.48	30.76 ($\uparrow 11.9\%$)	25.86	32.69 ($\uparrow 26.4\%$)
	ACC	0.72	0.71 ($\downarrow 0.01$)	0.73	0.68 ($\downarrow 0.05$)	0.72	0.68 ($\downarrow 0.04$)
CSP+SVM	ITR	19.56	28.66 ($\uparrow 46.5\%$)	19.90	28.18 ($\uparrow 41.6\%$)	19.72	25.16 ($\uparrow 27.6\%$)
	ACC	0.71	0.68 ($\downarrow 0.03$)	0.71	0.68 ($\downarrow 0.03$)	0.70	0.68 ($\downarrow 0.02$)

respectively. The best ITRs are marked in bold. Using FR in testing always improved the ITRs for both classifiers.

D. Computational Cost

The sampling rates of all three datasets were 250 Hz. We assumed that the BCI system brings in 10 sampling points ($L' = 10$) each time, i.e., we update the test trial every 40 ms. FRDW is required to complete all computations within 40 ms for real-time operations.

Table XIV shows the mean and standard deviation of the FRDW computation time for each update on MI1. All experiments were implemented via Python 3.8 and PyTorch, and ran on a server with NVIDIA RTX 3090 GPU and Intel(R)

Xeon(R) Gold 6226R 2.90GHz CPU. On average, FRDW always finished all computations within 40 ms, especially when EEGNet or CSP+SVM was used.

VI. CONCLUSIONS

MI is a classical and popular paradigm in EEG-based BCIs. Online accurate and fast decoding is very important to its successful applications. This paper has proposed a simple yet effective FRDW algorithm for this purpose. Dynamic windows enable the classification based on a test EEG trial shorter than those used in training, improving the decision speed; front-end replication fills a short test EEG trial to the length used in training, improving the classification accuracy. Within-

TABLE VI
AVERAGE ITRS AND ACCURACIES IN CROSS-SUBJECT CLASSIFICATION ON MI1.

Model	Training Data Augmentation												
	none				overlap				FR				
	FW	FRDW	EA+FW	EA+FRDW	FW	FRDW	EA+FW	EA+FRDW	FW	FRDW	EA+FW	EA+FRDW	
EEGNet	ITR	13.69	14.26 (↑4.2%)	19.40	27.83 (↑43.5%)	14.30	16.84 (↑17.8%)	19.78	26.97 (↑36.3%)	11.84	14.01 (↑18.3%)	18.22	26.37 (↑44.7%)
	ACC	0.37	0.36 (↓0.01)	0.41	0.40 (↓0.01)	0.37	0.36 (↓0.01)	0.42	0.40 (↓0.02)	0.36	0.35 (↓0.01)	0.41	0.39 (↓0.01)
CSP+Transformer	ITR	12.55	16.41 (↑30.8%)	16.67	25.00 (↑50.0%)	11.40	10.47 (↓8.2%)	15.70	23.42 (↑49.2%)	10.70	13.04 (↑21.9%)	17.40	27.47 (↑57.9%)
	ACC	0.38	0.36 (↓0.02)	0.41	0.39 (↓0.02)	0.37	0.33 (↓0.04)	0.41	0.39 (↓0.02)	0.37	0.35 (↓0.02)	0.43	0.41 (↓0.01)
CSP+SVM	ITR	13.19	15.94 (↑20.8%)	17.14	24.47 (↑42.8%)	12.90	14.84 (↑15.0%)	17.04	24.52 (↑43.9%)	12.83	14.78 (↑15.2%)	17.13	22.56 (↑31.7%)
	ACC	0.38	0.37 (↓0.01)	0.40	0.40 (-)	0.38	0.37 (↓0.01)	0.40	0.40 (-)	0.38	0.37 (-)	0.40	0.40 (-)

TABLE VII
AVERAGE ITRS AND ACCURACIES IN CROSS-SUBJECT CLASSIFICATION ON MI2.

Model	Training Data Augmentation												
	none				overlap				FR				
	FW	FRDW	EA+FW	EA+FRDW	FW	FRDW	EA+FW	EA+FRDW	FW	FRDW	EA+FW	EA+FRDW	
EEGNet	ITR	12.05	21.41 (↑77.9%)	8.08	12.41 (↑53.4%)	12.07	19.68 (↑63.1%)	12.27	15.14 (↑23.4%)	13.38	17.25 (↑28.9%)	12.10	13.47 (↑11.3%)
	ACC	0.61	0.63 (↑0.02)	0.61	0.61 (-)	0.63	0.63 (-)	0.64	0.63 (↓0.01)	0.63	0.63 (-)	0.63	0.62 (↓0.01)
CSP+Transformer	ITR	11.69	21.55 (↑84.4%)	9.94	13.19 (↑32.7%)	11.59	18.38 (↑58.6%)	9.74	13.95 (↑43.2%)	11.37	18.38 (↑61.7%)	11.22	17.68 (↑57.6%)
	ACC	0.62	0.61 (↓0.01)	0.63	0.61 (↓0.02)	0.60	0.61 (↑0.01)	0.64	0.62 (↓0.02)	0.61	0.61 (-)	0.64	0.64 (-)
CSP+SVM	ITR	10.05	12.75 (↑26.9%)	9.76	12.79 (↑31.1%)	9.79	13.64 (↑39.3%)	7.66	10.23 (↑33.6%)	9.06	11.57 (↑27.7%)	9.94	13.51 (↑35.9%)
	ACC	0.60	0.59 (↓0.01)	0.63	0.62 (↓0.01)	0.59	0.59 (-)	0.61	0.61 (-)	0.60	0.59 (↓0.01)	0.63	0.63 (-)

TABLE VIII
AVERAGE ITRS AND ACCURACIES IN CROSS-SUBJECT CLASSIFICATION ON MI3.

Model	Training Data Augmentation												
	none				overlap				FR				
	FW	FRDW	EA+FW	EA+FRDW	FW	FRDW	EA+FW	EA+FRDW	FW	FRDW	EA+FW	EA+FRDW	
EEGNet	ITR	20.51	33.63 (↑64.0%)	21.12	34.67 (↑64.2%)	21.44	31.51 (↑47.0%)	21.93	32.04 (↑46.1%)	21.89	34.32 (↑56.8%)	22.31	35.96 (↑61.2%)
	ACC	0.72	0.69 (↓0.03)	0.72	0.7 (↓0.02)	0.73	0.68 (↓0.05)	0.72	0.69 (↓0.04)	0.73	0.69 (↓0.04)	0.72	0.70 (↓0.02)
CSP+Transformer	ITR	19.37	25.53 (↑31.8%)	20.73	31.23 (↑50.7%)	19.60	26.73 (↑36.4%)	20.91	33.45 (↑60.0%)	18.90	26.48 (↑40.1%)	19.44	29.09 (↑49.6%)
	ACC	0.69	0.67 (↓0.02)	0.70	0.69 (↓0.01)	0.69	0.67 (↓0.02)	0.70	0.69 (↓0.01)	0.69	0.67 (↓0.02)	0.69	0.69 (↓0.01)
CSP+SVM	ITR	17.07	33.77 (↑97.8%)	18.05	31.89 (↑76.7%)	17.22	32.97 (↑91.5%)	17.87	31.37 (↑75.5%)	17.24	32.82 (↑90.4%)	17.92	32.11 (↑79.2%)
	ACC	0.69	0.68 (↓0.01)	0.70	0.68 (↓0.02)	0.69	0.68 (↓0.02)	0.70	0.68 (↓0.02)	0.69	0.67 (↓0.02)	0.70	0.69 (↓0.01)

subject and cross-subject online MI classification experiments on three public datasets, with three different classifiers and three different data augmentation approaches, demonstrated that FRDW can significantly increase the information transfer rate in MI decoding. Additionally, FR can also be used in training data augmentation. FRDW helped win national champion of the China BCI Competition in 2022.

REFERENCES

- [1] F. Lotte, L. Bougrain, A. Cichocki, M. Clerc, M. Congedo, A. Rakotomamonjy, and F. Yger, "A review of classification algorithms for EEG-based brain-computer interfaces: a 10 year update," *Journal of Neural Engineering*, vol. 15, no. 3, p. 031005, 2018.
- [2] A. Kübler, F. Nijboer, J. Mellinger, T. M. Vaughan, H. Pawelzik, G. Schalk, D. J. McFarland, N. Birbaumer, and J. R. Wolpaw, "Patients with ALS can use sensorimotor rhythms to operate a brain-computer interface," *Neurology*, vol. 64, pp. 1775–1777, 2005.
- [3] T. Vaughan, D. McFarland, G. Schalk, W. Sarnacki, D. Krusienski, E. Sellers, and J. Wolpaw, "The wadsworth BCI research and development program: at home with BCI," *IEEE Trans. on Neural Systems and Rehabilitation Engineering*, vol. 14, no. 2, pp. 229–233, 2006.
- [4] H. Yuan and B. He, "Brain-computer interfaces using sensorimotor rhythms: current state and future perspectives," *IEEE Trans. on Biomedical Engineering*, vol. 61, no. 5, pp. 1425–1435, 2014.
- [5] M. Steriade, "Cellular substrates of brain rhythms," *Electroencephalography: Basic Principles, Clinical Applications, and Related Fields*, vol. 5, pp. 31–83, 2005.
- [6] G. Pfurtscheller, C. Brunner, A. Schlögl, and F. L. Da Silva, "Mu rhythm (de) synchronization and EEG single-trial classification of different motor imagery tasks," *NeuroImage*, vol. 31, no. 1, pp. 153–159, 2006.
- [7] G. Pfurtscheller and C. Neuper, "Future prospects of ERD/ERS in the context of brain-computer interface (BCI) developments," *Progress in Brain Research*, vol. 159, pp. 433–437, 2006.
- [8] C. Neuper, M. Wörtz, and G. Pfurtscheller, "ERD/ERS patterns re-

TABLE IX
 PAIRED-SAMPLE t -TEST RESULTS ON THE TEST ITRS IN TABLES III-V BETWEEN FW AND FRDW.

Model	Training Data Augmentation								
	none			overlap			FR		
	MI1	MI2	MI3	MI1	MI2	MI3	MI1	MI2	MI3
EEGNet	0.058	0.007	0.039	0.079	0.232	0.074	0.040	0.034	0.075
CSP+Transformer	0.057	0.162	0.067	0.065	0.017	0.263	0.041	0.049	0.073
CSP+SVM	0.079	0.072	0.098	0.060	0.110	0.106	0.050	0.049	0.232

TABLE X
 PAIRED-SAMPLE t -TEST RESULTS ON THE TEST ITRS IN TABLES VI AND VIII BETWEEN FW AND FRDW.

Model	Training Data Augmentation																	
	none w/o EA			none w/ EA			overlap w/o EA			overlap w/ EA			FR w/o EA			FR w/ EA		
	MI1	MI2	MI3	MI1	MI2	MI3	MI1	MI2	MI3	MI1	MI2	MI3	MI1	MI2	MI3	MI1	MI2	MI3
EEGNet	0.641	0.074	0.007	0.077	0.094	0.053	0.176	0.149	0.232	0.013	0.170	0.053	0.085	0.035	0.034	0.079	0.099	0.041
CSP+Transformer	0.134	0.234	0.162	0.080	0.168	0.061	0.527	0.185	0.017	0.059	0.023	0.043	0.322	0.089	0.049	0.014	0.087	0.377
CSP+SVM	0.241	0.278	0.072	0.028	0.037	0.066	0.192	0.291	0.110	0.020	0.020	0.063	0.182	0.281	0.049	0.034	0.029	0.060

TABLE XI
 PAIRED-SAMPLE t -TEST RESULTS ON THE TEST ITRS IN TABLES VI AND VIII FOR FRDW WITHOUT EA AND WITH EA.

Model	Dataset	Training Data Augmentation		
		none	overlap	FR
EEGNet	MI1	0.089	0.040	0.075
	MI2	0.199	0.381	0.324
	MI3	0.299	0.758	0.591
CSP+Transformer	MI1	0.919	0.021	0.007
	MI2	0.399	0.489	0.891
	MI3	0.032	0.069	0.377
CSP+SVM	MI1	0.029	0.039	0.075
	MI2	0.996	0.681	0.751
	MI3	0.519	0.636	0.832

TABLE XII
 AVERAGE PERFORMANCE WITHOUT AND WITH FR IN TESTING, WHEN CSP+TRANSFORMER WAS USED ON MI1.

Metric	Training Data Augmentation					
	none		overlap		FR	
	w/o FR	w/ FR	w/o FR	w/ FR	w/o FR	w/ FR
ACC	0.53	0.53	0.52	0.52	0.55	0.55
ITR	55.16	57.18	54.96	56.76	58.73	61.87
Time (s)	0.39	0.38	0.36	0.36	0.40	0.39

flecting sensorimotor activation and deactivation,” *Progress in Brain Research*, vol. 159, pp. 211–222, 2006.

- [9] M. Lotze and U. Halsband, “Motor imagery,” *Journal of Physiology-paris*, vol. 99, no. 4–6, pp. 386–395, 2006.
- [10] D. Coyle, J. Garcia, A. R. Satti, and T. M. McGinnity, “EEG-based continuous control of a game using a 3 channel motor imagery BCI game,” in *IEEE Symposium on Computational Intelligence, Cognitive Algorithms, Mind, and Brain*, vol. 1–7, Paris, France, Apr. 2011.
- [11] K. LaFleur, K. Cassady, A. Doud, K. Shades, E. Rogin, and B. He, “Quadcopter control in three-dimensional space using a noninvasive motor imagery-based brain–computer interface,” *Journal of Neural Engineering*, vol. 10, no. 4, p. 046003, 2013.
- [12] Á. Fernández-Rodríguez, F. Velasco-Álvarez, and R. Ron-Angevin, “Review of real brain-controlled wheelchairs,” *Journal of Neural En-*

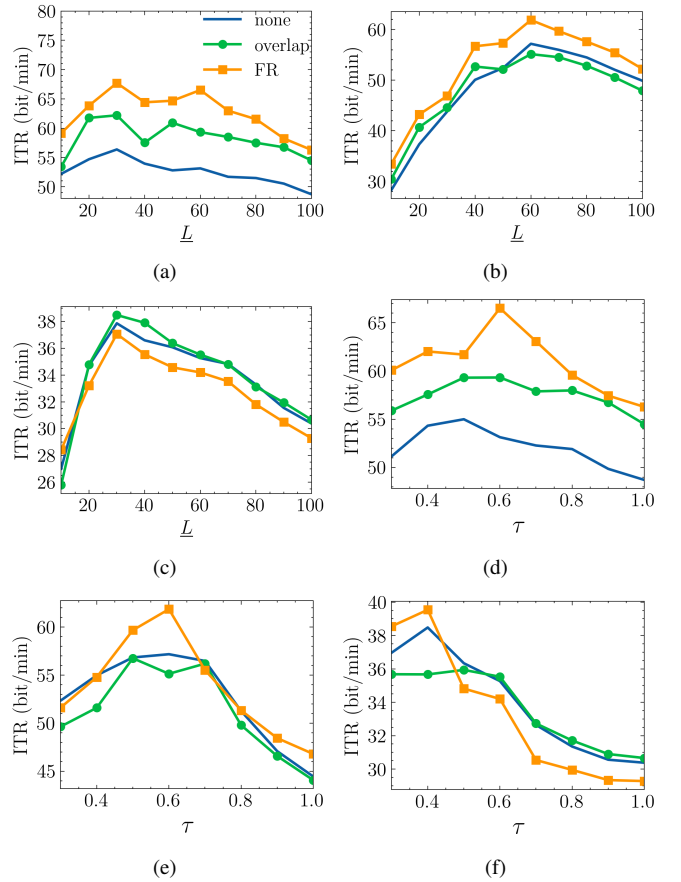


Fig. 2. Sensitivity analysis on MI1 for within-subject classification. (a)–(c) ITR w.r.t. different \underline{L} ($\tau = 0.6$) on EEGNet, CSP+Transformer and CSP+SVM, respectively; (d)–(f) ITR w.r.t. different τ ($\underline{L} = 60$) on EEGNet, CSP+Transformer and CSP+SVM, respectively.

gineering, vol. 13, no. 6, p. 061001, 2016.

- [13] R. Ron-Angevin, F. Velasco-Álvarez, Á. Fernández-Rodríguez, A. Díaz-Estrella, M. J. Blanca-Mena, and F. J. Vizcaíno-Martín, “Brain-computer interface application: auditory serial interface to control a two-class motor-imagery-based wheelchair,” *Journal of Neuroengineering and*

TABLE XIII
AVERAGE PERFORMANCE WITHOUT AND WITH FR IN TESTING, WHEN
CSP+SVM WAS USED ON M11.

Metric	Training Data Augmentation					
	none		overlap		FR	
	w/o FR	w/ FR	w/o FR	w/ FR	w/o FR	w/ FR
ACC	0.46	0.46	0.46	0.46	0.46	0.46
ITR	35.11	35.27	35.26	35.53	33.94	34.20
Time (s)	0.36	0.36	0.35	0.35	0.36	0.36

TABLE XIV
COMPUTATION TIME (MS) OF FRDW.

Model	Training Data Augmentation	FRDW	
		Mean	Std
EEGNet	none	12.7	2.8
	overlap	12.7	2.7
	FR	12.5	2.6
CSP+Transformer	none	20.3	16.3
	overlap	22.6	16.7
	FR	20.1	17.9
CSP+SVM	none	2.8	2.8
	overlap	3.9	2.5
	FR	4.3	2.9

Rehabilitation, vol. 14, no. 1, pp. 1–16, 2017.

- [14] E. López-Larraz, A. Sarasola-Sanz, N. Irastorza-Landa, N. Birbaumer, and A. Ramos-Murguialday, “Brain-machine interfaces for rehabilitation in stroke: a review,” *NeuroRehabilitation*, vol. 43, no. 1, pp. 77–97, 2018.
- [15] H. He and D. Wu, “Transfer learning for brain–computer interfaces: A Euclidean space data alignment approach,” *IEEE Trans. on Biomedical Engineering*, vol. 67, no. 2, pp. 399–410, 2019.
- [16] F. Lotte and C. Guan, “Regularizing common spatial patterns to improve BCI designs: unified theory and new algorithms,” *IEEE Trans. on Biomedical Engineering*, vol. 58, no. 2, pp. 355–362, 2010.
- [17] M. Arvaneh, C. Guan, K. K. Ang, and C. Quek, “Optimizing the channel selection and classification accuracy in EEG-based BCI,” *IEEE Trans. on Biomedical Engineering*, vol. 58, no. 6, pp. 1865–1873, 2011.
- [18] H. Wang, Q. Tang, and W. Zheng, “L1-norm-based common spatial patterns,” *IEEE Trans. on Biomedical Engineering*, vol. 59, no. 3, pp. 653–662, 2011.
- [19] W. Samek, M. Kawanabe, and K.-R. Müller, “Divergence-based framework for common spatial patterns algorithms,” *IEEE Reviews in Biomedical Engineering*, vol. 7, pp. 50–72, 2013.
- [20] W. Wu, Z. Chen, X. Gao, Y. Li, E. N. Brown, and S. Gao, “Probabilistic common spatial patterns for multichannel EEG analysis,” *IEEE Trans. on Pattern Analysis and Machine Intelligence*, vol. 37, no. 3, pp. 639–653, 2014.
- [21] K. K. Ang, Z. Y. Chin, H. Zhang, and C. Guan, “Filter bank common spatial pattern (FBCSP) in brain-computer interface,” in *IEEE Int’l Joint Conf. on Neural Networks*, Hong Kong, China, Jun. 2008, pp. 2390–2397.
- [22] C. Kim, J. Sun, D. Liu, Q. Wang, and S. Paek, “An effective feature extraction method by power spectral density of EEG signal for 2-class motor imagery-based BCI,” *Medical & Biological Engineering & Computing*, vol. 56, pp. 1645–1658, 2018.
- [23] M. N. Alam, M. I. Ibrahimy, and S. Motakabber, “Feature extraction of eeg signal by power spectral density for motor imagery based bci,” in *IEEE Int’l Conf. on Computer and Communication Engineering*, Kuala Lumpur, Malaysia, Jun. 2021, pp. 234–237.
- [24] B. Xu, L. Zhang, A. Song, C. Wu, W. Li, D. Zhang, G. Xu, H. Li, and H. Zeng, “Wavelet transform time-frequency image and convolutional network-based motor imagery EEG classification,” *IEEE Access*, vol. 7, pp. 6084–6093, 2018.
- [25] V. J. Lawhern, A. J. Solon, N. R. Waytowich, S. M. Gordon, C. P. Hung, and B. J. Lance, “EEGNet: a compact convolutional neural network for EEG-based brain–computer interfaces,” *Journal of Neural Engineering*, vol. 15, no. 5, p. 056013, 2018.
- [26] R. T. Schirmer, J. T. Springenberg, L. D. J. Fiederer, M. Glasstetter, K. Eggenberger, M. Tangermann, F. Hutter, W. Burgard, and T. Ball, “Deep learning with convolutional neural networks for EEG decoding and visualization,” *Human Brain Mapping*, vol. 38, no. 11, pp. 5391–5420, 2017.
- [27] T. M. Ingolfsson, M. Hersche, X. Wang, N. Kobayashi, L. Cavigelli, and L. Benini, “EEG-TCNet: An accurate temporal convolutional network for embedded motor-imagery brain–machine interfaces,” in *IEEE Int’l Conf. on Systems, Man, and Cybernetics*, Toronto, Ontario, Oct. 2020, pp. 2958–2965.
- [28] Y. K. Musallam, N. I. AlFassam, G. Muhammad, S. U. Amin, M. Al-sulaiman, W. Abdul, H. Altaheri, M. A. Bencherif, and M. Algabri, “Electroencephalography-based motor imagery classification using temporal convolutional network fusion,” *Biomedical Signal Processing and Control*, vol. 69, p. 102826, 2021.
- [29] H. Altaheri, G. Muhammad, and M. Al-sulaiman, “Physics-informed attention temporal convolutional network for EEG-based motor imagery classification,” *IEEE Trans. on Industrial Informatics*, vol. 19, no. 2, pp. 2249–2258, 2022.
- [30] K. Liu, M. Yang, Z. Yu, G. Wang, and W. Wu, “FBMSNet: A filter-bank multi-scale convolutional neural network for EEG-based motor imagery decoding,” *IEEE Trans. on Biomedical Engineering*, vol. 70, no. 2, pp. 436–445, 2023.
- [31] Y. Fengwei, C. Peng, X. Kai, P. Hualin, and L. Xueyin, “Online classification method for motor imagery EEG with spatial information,” *Journal of System Simulation*, vol. 35, no. 2, p. 254, 2023.
- [32] Z. Tayeb, J. Fedjaev, N. Ghaboosi, C. Richter, L. Everding, X. Qu, Y. Wu, G. Cheng, and J. Conrath, “Validating deep neural networks for online decoding of motor imagery movements from EEG signals,” *Sensors*, vol. 19, no. 1, p. 210, 2019.
- [33] P. K. Parashiva and A. Vinod, “Improving direction decoding accuracy during online motor imagery based brain-computer interface using error-related potentials,” *Biomedical Signal Processing and Control*, vol. 74, p. 103515, 2022.
- [34] R. Kus, D. Valbuena, J. Zygierevicz, T. Malechka, A. Graeser, and P. Durka, “Asynchronous BCI based on motor imagery with automated calibration and neurofeedback training,” *IEEE Trans. on Neural Systems and Rehabilitation Engineering*, vol. 20, no. 6, pp. 823–835, 2012.
- [35] J. Choi, K. T. Kim, J. H. Jeong, L. Kim, S. J. Lee, and H. Kim, “Developing a motor imagery-based real-time asynchronous hybrid BCI controller for a lower-limb exoskeleton,” *Sensors*, vol. 20, no. 24, p. 7309, 2020.
- [36] C. Yang, X. Han, Y. Wang, R. Saab, S. Gao, and X. Gao, “A dynamic window recognition algorithm for SSVEP-based brain–computer interfaces using a spatio-temporal equalizer,” *International Journal of Neural Systems*, vol. 28, no. 10, p. 1850028, 2018.
- [37] Y. Chen, C. Yang, X. Chen, Y. Wang, and X. Gao, “A novel training-free recognition method for SSVEP-based BCIs using dynamic window strategy,” *Journal of Neural Engineering*, vol. 18, no. 3, p. 036007, 2021.
- [38] H. Habibzadeh, J. J. S. Norton, T. M. Vaughan, T. Soyata, and D.-S. Zois, “A voting-enhanced dynamic-window-length classifier for SSVEP-based BCIs,” *IEEE Trans. on Neural Systems and Rehabilitation Engineering*, vol. 29, pp. 1766–1773, 2021.
- [39] W. Zhou, A. Liu, L. Wu, and X. Chen, “A L1 normalization enhanced dynamic window method for SSVEP-based BCIs,” *Journal of Neuroscience Methods*, vol. 380, p. 109688, 2022.
- [40] H. Yin, Z. Ji, Z. Lian, Y. Yang, N. Liu, and H. Wang, “Application of kurtosis based dynamic window to enhance SSVEP recognition,” in *China Automation Congress*, Xiamen, China, Nov. 2022, pp. 571–576.
- [41] W. Zhou, A. Liu, and X. Chen, “Compact CNN with dynamic window for SSVEP-based BCIs,” in *Chinese Control Conference*, Hefei, China, Jul. 2022, pp. 3097–3101.
- [42] D. Wu, X. Jiang, and R. Peng, “Transfer learning for motor imagery based brain-computer interfaces: A tutorial,” *Neural Networks*, vol. 153, pp. 235–253, 2022.
- [43] M. Tangermann, K.-R. Müller, A. Aertsen, N. Birbaumer, C. Brunner, C. Brunner, R. Leeb, C. Mehring, K. J. Miller, G. Mueller-Putz *et al.*, “Review of the BCI competition IV,” *Frontiers in Neuroscience*, vol. 6, p. 55, 2012.
- [44] A. Vaswani, N. Shazeer, N. Parmar, J. Uszkoreit, L. Jones, A. N. Gomez, Ł. Kaiser, and I. Polosukhin, “Attention is all you need,” in *Proc. Advances in Neural Information Processing Systems*, vol. 30, Los Angeles, CA, Dec. 2017.

- [45] Y. Song, Q. Zheng, B. Liu, and X. Gao, "EEG Conformer: Convolutional transformer for EEG decoding and visualization," *IEEE Trans. on Neural Systems and Rehabilitation Engineering*, vol. 31, pp. 710–719, 2022.
- [46] Y. Song, X. Jia, L. Yang, and L. Xie, "Transformer-based spatial-temporal feature learning for EEG decoding," *arXiv preprint arXiv:2106.11170*, 2021.
- [47] J. A. K. Suykens and J. Vandewalle, "Least squares support vector machine classifiers," *Neural Processing Letters*, vol. 9, pp. 293–300, 1999.